

## INVESTIGATING LIGHT PROPAGATION IN FULL AND SKIMMED MILK BASED ON SPECTROSCOPY AND MONTE CARLO ANALYSIS

N. A. I. MUHAMAD KAMIL<sup>1</sup>, I. H. ZAKARIA<sup>2</sup>, W. Z. WAN ISMAIL<sup>1\*</sup>,  
I. ISMAIL<sup>1</sup>, J. JAMALUDIN<sup>1</sup>, S. R. BALAKRISHNAN<sup>1</sup>, M. SAHRIM<sup>1</sup>

### ABSTRACT

Milk quality can be determined through its fat composition. It is important to know the fat composition in milk to ensure consumption of the right product for health reasons. Spectroscopy can be used to study the fat composition in milk. In this paper, light propagation in milk based on visible and near infrared (NIR) spectra is investigated. Samples comprise skimmed and full milk. Full milk shows higher absorbance at visible (VIS) spectra compared to skimmed milk. The analysis on NIR spectra also shows that full milk has higher absorbance peak than skimmed milk due to higher amount of fat globule. Fourier-transform infrared spectroscopy (FTIR) analysis is done to study the chemical compounds such as C=C and O-H in milk samples. Through FTIR, the unsaturated fatty acid and water element in the samples were analyzed. Both milk samples show higher water element than carbon. Numerical modeling based on Monte Carlo method is also done to support experimental results. The modeling results show that full milk has a larger photon count compared to skimmed milk. This is attributed to the large fat globule in full milk that has higher absorbance over skimmed milk. Thus, characterization of milk fat based on spectroscopy techniques can monitor milk adulteration issues, which indirectly gives us guidance on healthy dairy intakes.

**KEYWORDS:** Absorbance, Transmittance, Milk fat, Monte Carlo, Spectroscopy, Photon count and photon loss.

### 1. INTRODUCTION

Light propagation consists of three main light phenomena: absorption, scattering and transmission [1]. Based on [2], light absorption refers to the disappearance of photon after hitting a particle, whereas light scattering involves changes in photon direction when light hits particle or molecule, as shown in Fig. 1. Transmission intensity,  $I$

---

<sup>1</sup> Member, Advanced Devices and Systems, Department of Electrical and Electronics Engineering, Faculty of Engineering and Built Environment, Universiti Sains Islam, Malaysia.

<sup>2</sup> Engineer, Berrybak Sdn. Bhd., George Town, Penang, Malaysia.

\* Corresponding Author: [drwanzakiah@usim.edu.my](mailto:drwanzakiah@usim.edu.my)

decreases for both absorbed and scattered light. The attenuation due to absorption can be found using Eq. (1). Then, the attenuation due to scattering can be measured using Eq. (2) where  $I_0$ ,  $\alpha$ , and  $\tau$  are the incident intensity before attenuation, absorption coefficient and turbidity respectively [2]. The light absorbance can be calculated using  $\log I_0/I$  or  $\log(1/T)$ .  $T$  refers to light transmittance.

$$I = I_0 \cdot 10^{-\alpha x} \quad (1)$$

$$I = I_0 \cdot e^{-\tau x} \quad (2)$$

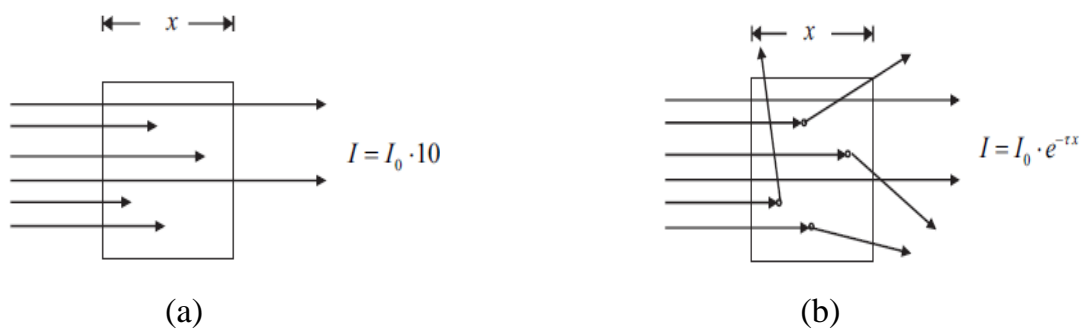


Fig. 1. Transmitted light disturbed by either (a) absorbance (b) scattering [2].

The exposure of a turbid medium to the light source causes the medium to change to hazy and cloudy states due to the presence of the insoluble and suspended medium. The high opaqueness of a medium causes the medium to become more turbid with high degradable of light intensity. Turbidity is an important parameter to measure the quality of liquid, providing a wide range of applications for mankind. Recent water quality monitoring system applies Internet of Things (IOT) [3].

Milk, the most consumed dairy product in the world, is an example of turbid media. Fat, carbohydrates, proteins and mineral contents in milk are important to develop a growth-mechanism effect and well-nourishes diet for mankind. Nevertheless, the role of milk as a nutritious food is questioned as the composition of milk has been altered results in health problems. Full milk composition is being altered by adding water to increase milk volume, indirectly affecting the milk's quality [4-6].

Spectroscopy is widely applied to monitor food quality. The authentication of raw milk from reconstituted milk using FTIR spectroscopy [5] is done. The effectiveness of mid-infrared spectrometer is analyzed and results show mineral compositions of bulk milk [6]. Many spectroscopic analyses are done on milk samples to characterize milk fat including Laser spectroscopy [7], Fiber-optic spectroscopy [8], MEMS-based Fourier Transform Infra-Red (FTIR) spectrometer sensing [9] and Raman spectroscopy [10]. There are many applications based on spectroscopy analysis such as the use of Fourier Transform Infra-Red (FTIR) to identify the mineral drug substance (purified bentonite) in a drug product [11] and to analyze the chemical properties of “*Nicotiana Plumbginifolia*” as an important element in ethnomedicine [12].

Light propagation in milk samples can be modelled based on Monte Carlo technique. Monte Carlo method applies the stochastic model that analyzes the random probability distribution or pattern which is not precisely predicted [13]. Monte Carlo (MC) algorithm offers a randomized statistical sampling to solve the complex structure in milk composition and are widely used to study biological materials such as human tissues [1].

Previous spectroscopy studies of milk samples focus on experimental or theoretical technique and only one type of spectrometer is utilized. Hence, this research aims to investigate light propagation in milk samples based on experimental and theoretical studies. Three spectroscopy techniques are applied and modeling is done based on Monte Carlo simulation. Two types of milks are compared and analyzed based on their optical properties. Full milk shows higher light absorption than skimmed milk because of larger fat content in it.

## **2. MATERIALS AND METHODS**

### **2.1 Materials and Experimental Set Up**

Three different types of spectrometers are used such as Ocean Optic Flame Near-Infrared (NIR) Spectrometer, Perkin Elmer Lambda 750 UV/VIS/NIR Spectrometer and Varian 3100 Excalibur Series Fourier Transform Infra-Red (FTIR) Spectrometer. These

spectrometers are used as they can offer large size sampling, cost-effective, fast and reliable measurement.

## 2.2 Sample Preparations

Ultra-High Temperature (UHT) milk samples consist of skimmed and full milk from brand 'Dutch Lady'. Firstly, both samples are diluted with a ratio of 1:100 for water and milk respectively. Distilled water is used as a reference and comparison with milk samples. A prepared sample is placed in the 10 mm plastic cuvette and lightly shaken and stirred to mix the solution before being placed in Ocean Optic Flame Near-Infrared (NIR) Spectrometer and Perkin Elmer Lambda 750 UV/VIS/NIR Spectrometer at spectrum ranges of 950-1650 nm and 350-860 nm respectively. A droplet of undiluted solution from both milk samples are tested in a Varian 3100 Excalibur Series for FTIR spectroscopy. The FTIR spectroscopy is used to identify and differentiate any chemical compounds in both samples. The wavelength ranges for FTIR Spectroscopy are from 550 to 3950  $\text{cm}^{-1}$  with the analysis is done in Varian Resolution Software. The experiments are repeated 5 times to ensure consistency and accuracy of the measurement. The output is averaged out with the standard deviation  $\sim 0.01-0.03$ .

## 2.3 Theoretical Analysis

Many modeling techniques can be applied to analyze the light propagation in random media such as Monte Carlo [14-19], Finite Element Modeling (FEM) [20] and Finite Different Time Domain (FDTD) [21]. Vaskova *et al.* [10] state that mathematical evaluation can be used to measure the accurate milk fat content for the quality control of the milk product. Here, Monte Carlo modeling technique is used to simulate the photon count and photon loss in milk. The selected technique can be used to observe the amount of photon transmitted and loss in skimmed and full milk where the scattering factors such as internal coefficient, anisotropic parameters and forward power are analyzed. Besides that, Monte Carlo can track the movement of photons inside the samples which experience absorption, scattering and power loss. Fundamentally, the

photon propagation is initiated by photon launching followed by photon absorption, scattering and is terminated by photon detection as depicted in Fig. 2.

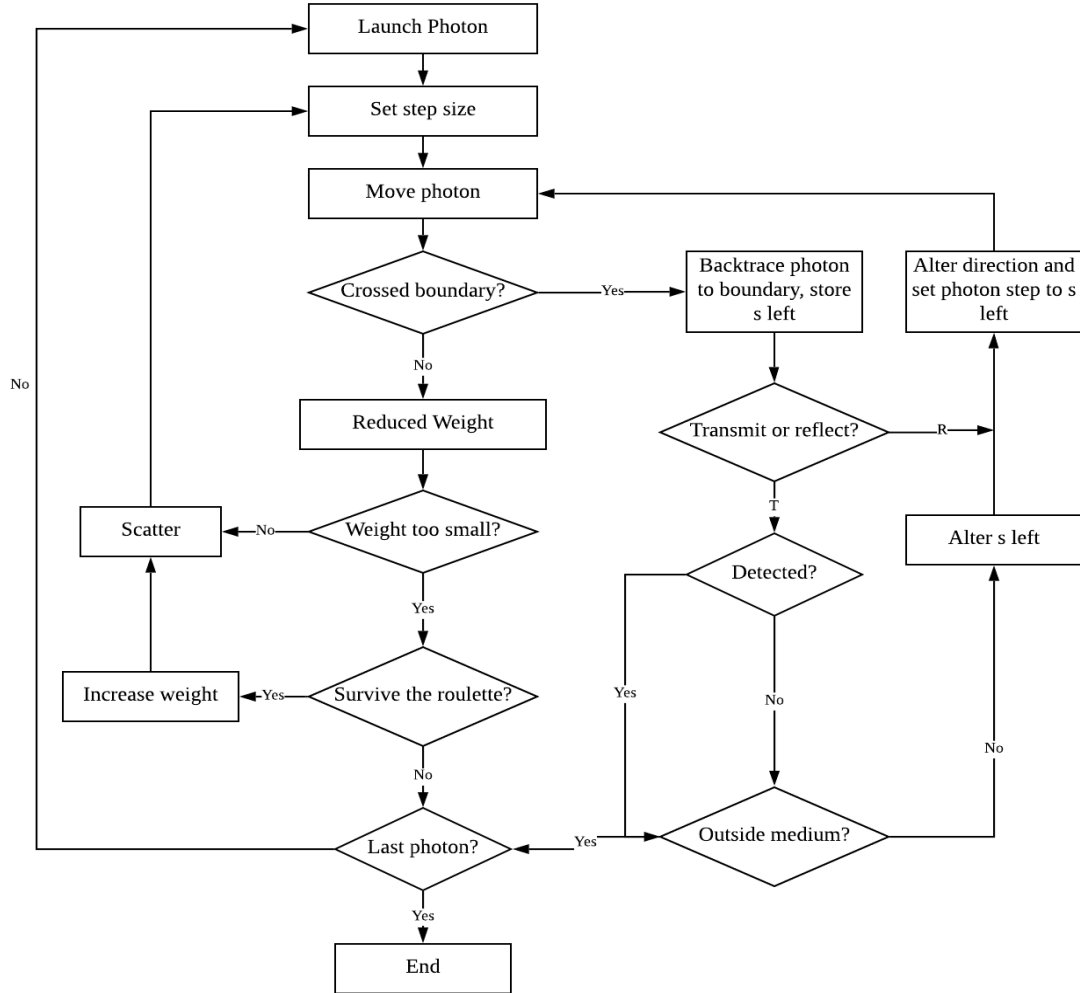


Fig. 2. Modeling of light propagation based on Monte Carlo technique [17].

In Monte Carlo modeling technique, four main steps are involved; photon launching, photon absorption, photon scattering and finally, photon detection with continuous propagation [14].

### 2.3.1 Photon initialization

At the first stage, the photon is launched, followed by the step length expressed by Eq. (3) [15].

$$\Delta s = \frac{-\ln(rnd)}{\mu_t} \tag{3}$$

While  $\mu_t$  refers to internal coefficient,  $rnd$  is a random number that is launched between the interval of 0 and 1 and will be sampled at every executing loop,  $\mu_a$  is the absorption coefficient and,  $\mu_s$  is the scattering coefficient as shown in Eq. (4) [16].

$$\mu_t = \mu_s + \mu_a \quad (4)$$

At the same time, virtual weight is assigned to each photon before any movement. The first photon position exists at 3D space,  $(x_1, y_1, z_1)$ . The first polar position at 3D space is given by Eq. (5) [15].

$$\begin{aligned} x_1 &= x_0 + \mu_x \Delta s \\ y_1 &= y_0 + \mu_y \Delta s \\ z_1 &= z_0 + \mu_z \Delta s \end{aligned} \quad (5)$$

### 2.3.2 Photon absorption

The second stage involves photon absorption. After the absorption, photon reduces its weight ( $w$ ) by setting the threshold for every iteration. The reduction of photon weight is given by Eq. (6) [16].

$$w_i = w_{i-1} \left(1 - \frac{\mu_a}{\mu_t}\right) \text{ where } i = 1, 2, 3, \dots \quad (6)$$

Russian roulette technique is used in the modeling because the sole calculation time to estimate the light propagation is not realistic. Thus, random value ( $rnd$ ) is set based on Eq. (7) [16].

$$rnd = \frac{w_0}{10} \quad (7)$$

Where  $w_0$  refers to the initial photon weight. If the random number exceeds the threshold value, the photon will be terminated, photon weight is increased by  $1/p$ .

### 2.3.3 Photon scattering and propagation

The third stage consists of photon scattering and propagation. When photon reduces its weight, but still alive in the roulette, they can be scattered. Hence, at this stage, the deflection angle can be measured based on the phase function. Deflection angle,  $\theta$  is calculated based on Eqs. 8 and 9 [16].

$$\theta = \cos^{-1} \left[ \frac{1}{2g} \cdot \left\{ 1 + g^2 - \left( \frac{rnd}{H} + (1 + g^{-2\alpha})\alpha^{-1} \right) \right\} \right] \quad (8)$$

$$\text{Where: } H = \frac{(1+g^2)^{2\alpha}}{(1+g)^{2\alpha} - (1-g)^{2\alpha}} \quad (9)$$

Where  $g$  is the anisotropy factor referring to scattering function,  $H$  is Henvey-Greenstein phase function and  $\alpha$  is the weight factor. The new position  $(x_1, y_1, z_1)$  can be generated using the obtained phase function, deflection angle and the azimuthal angle,  $\psi$ .  $\psi$  is randomly chosen from the uniform distribution within the interval of  $(0, 2\pi)$ , expressed by Eqs. (10-12) [16].

$$x_{i+1} = x_i + \Delta s \cdot \left( \frac{\sin(\theta)}{\sqrt{1-u_z^2}} (u_x \cdot u_z \cdot \cos(\varphi) \quad u_y \cdot \sin(\varphi) \quad u_x \cdot \cos(\theta)) \right) \quad (10)$$

$$y_{i+1} = y_i + \Delta s \cdot \left( \frac{\sin(\theta)}{\sqrt{1-u_z^2}} (u_y \cdot u_z \cdot \cos(\varphi) \quad u_x \cdot \sin(\varphi)) \quad u_y \cdot \cos(\theta) \right) \quad (11)$$

$$z_{i+1} = z_i + \Delta s \cdot (-\sin(\theta) \cdot \cos(\varphi) \cdot \sqrt{1-u_z^2} + u_z \cdot \cos(\theta)) \quad (12)$$

where,  $(u_x, u_y, u_z)$  represents the values of photon propagation in every iteration,  $i$ .

### 2.3.4 Photon detection

The photon is detected at the final stage. Photon detection is done by considering its weight and the optical properties of the measured medium such as refractive index, number of emitted photon, position, absorption coefficient and scattering coefficient [17]. Table 1 shows the weight of milk fat contents, scattering coefficient and absorption coefficient. The parameters in the table are used to record backscattered count and photon loss during scattering process. The internal coefficient is determined from Eq. (4) whereas the scattering and absorption coefficients are based on Qin et al. [26].

Table 1. Scattering, absorption and internal coefficients for both milk samples.

Type of medium	Weight of Milk Fat Contents, gram (g)	Scattering coefficient, $\mu_s$	Absorption Coefficient, $\mu_a$	Internal Coefficient, $\mu_t$
Skimmed Milk	0.0	1.65	0.55	2.20
	0.1	1.68	0.56	2.24
Full Milk	3.2	2.36	1.80	4.16
	3.8	2.36	1.9	4.26

Here, modeling is used to support experimental analysis in terms of light or photon transmitted in milk, not as a direct comparison with the experimental results.

### **3. RESULTS AND DISCUSSION**

The experiments are done using various spectrometer techniques whereas the theoretical analysis is done based on Monte Carlo modeling.

#### **3.1 Experimental Analysis**

The experimental analysis is carried out based on Visible (VIS), Near Infra-Red (NIR) and Infra-Red (IR) spectra.

##### **3.1.1 Visible (VIS) spectrum**

Figure 3(a) shows the absorbance spectra of skimmed milk, full milk and water from 380 nm – 860 nm. The spectra are plotted using UV WinLab software in Perkin Elmer Lambda, 750 UV/VIS/NIR Spectroscopy. The samples in Visible (VIS) spectrum are analyzed based on spectrum continuity [18] instead of observing the milk fat spectrum at certain peaks, as analyzed in Near Infra-Red (NIR) and Infra-Red (IR) spectra [9, 10, 19, 22]. It is clearly shown that the absorbance of the skimmed milk is much lower than full milk. The almost linear line is observed for water sample due to weak light absorbance in the visible spectrum compared to Near Infra-Red (NIR) and Infra-Red (IR) spectra.

##### **3.1.2 Near infra-red (NIR) spectrum**

Figure 3(b) shows the absorbance spectra for skimmed milk, full milk and water from 960 -1660 nm using Optic NIR Spectrometer. From the fig., we observe that the absorbance of full milk shows higher absorbance over skimmed milk and water respectively. The three strong absorption peaks observed at 972, 1158 and 1392 nm in the NIR spectrum. In Fig. 3.2(b), the absorbance shows negative values from 1050 nm until 1100 nm which we attribute that to the background noise and spectrometer calibration.



## INVESTIGATING LIGHT PROPAGATION IN FULL AND SKIMMED MILK...

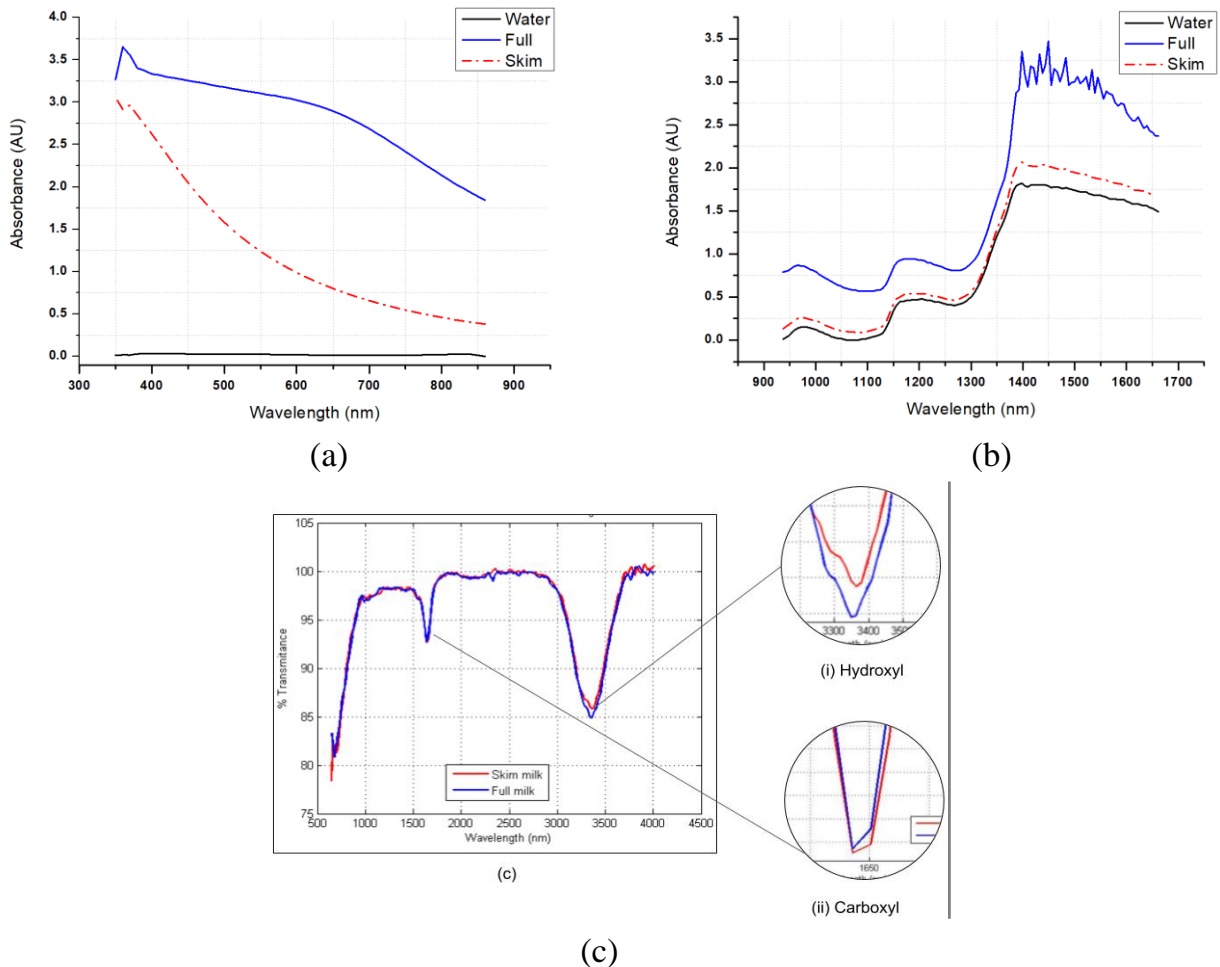


Fig. 3. Spectrum analysis of different milk samples (a) Visible (VIS) spectrometer versus wavelength (b) Near infra-red (NIR) absorbance versus wavelength (c) FTIR transmittance versus wavelength.

### 3.1.3 Fourier transform infra-red (FTIR) spectrum

Investigating light propagation in milk is continued using Fourier Transform Infra-Red (FTIR) spectroscopy. Transmission spectra for both milk samples are shown in Fig. 3(c). The fig. shows the transmission of two main functional groups in milk samples, hydroxyl and carboxyl group. A small valley from 1500-1680 nm represents alkene (chemical bond, C=C) and a broad valley from 3300 - 3500 nm represents hydroxyl (chemical bond, O-H) groups. The C, O and H refer to carbon, oxygen and hydrogen respectively. A broad hydroxyl spectrum (O-H) is observed from the graph due to high water composition in the samples. The dominated water bands in the spectra can affect the absorption of other milk fat components such as triglycerides and saturated

fatty acid [22]. We observe slight changes at alkene (C=C) stretch that is attributed to the unsaturated fatty acid which characterizes skimmed and full milk [9, 10, 22].

In addition, strong water (O-H) absorption was observed at 960, 1440 and 1950 nm using MEMs spectrometer [9] whereas Raman spectroscopy was used to characterize milk fat consist of triglycerides groups, saturated and unsaturated fatty acid. The characterization is based on chemical bonds C=O, CH<sub>2</sub> and C=C stretching. The functional groups based on absorbance wavelength are summarized in Table 2.

Table 2. Chemical compounds at varied wavelength ranges in FTIR analysis.

Wavelength Peak/ Ranges (cm <sup>-1</sup> )	Functional Group	Chemical Bonds	Types of Chemical Compounds
3300 – 3500	Hydroxyl	O-H	Water
1500-1680	Alkene	C=C	Unsaturated fatty acid

### 3.2 Theoretical Analysis

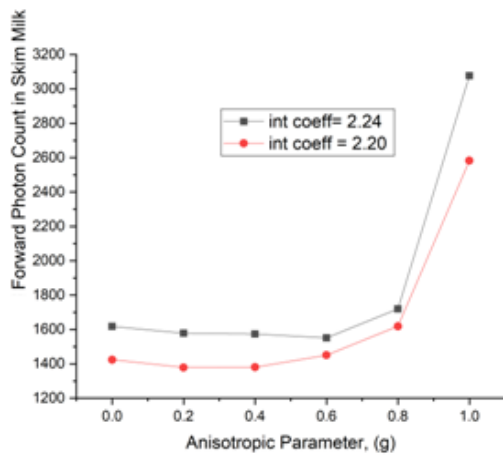
The Monte Carlo technique is used to measure the forward photon count for different anisotropy values,  $g$  in both skimmed and full milk. Henvey-Greenstein suggests three main scattering types based on anisotropic value,  $g$  where purely forward scattering exists for  $g=1$ , while purely backscattering and isotropic scattering exist for  $g=-1$  and  $g=0$  respectively [23].

Henvey-Greenstein phase function is commonly used to analyze the light scattering in biomedical fields such as tissues and cell [14, 24] where most of biological tissues have anisotropic value,  $g$  greater than 0.7 ( $g>0.7$ ) [25]. Hence, forward scattering in the range of  $0<g<1$  is applied to analyze the milk fat due to the disordered and random media [26].

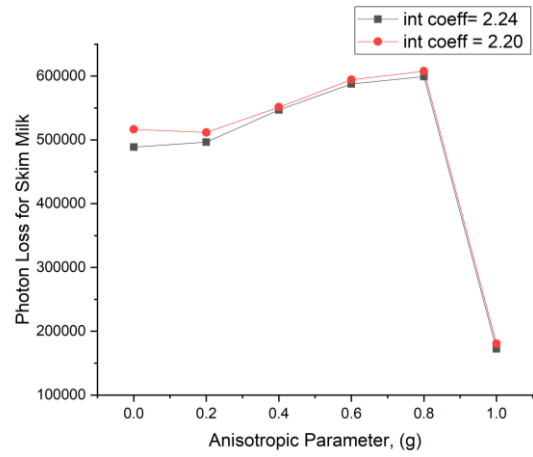
Numerical modeling based on Monte Carlo technique is shown in Fig. 4. Different internal coefficients are measured to observe their effects on various anisotropic parameters. The forward photon count in skimmed milk are measured and compared using internal coefficient of 2.24 and 2.20 respectively (Fig. 4(a) and 4(b)). Meanwhile, Fig. 4(c) and 4(d) show photon count and photon loss for both samples based on various anisotropy parameters. High forward power is analyzed when high internal coefficient is applied to the skimmed milk. Besides that, there is a high incline

when  $g$  parameters approach 1 for both internal coefficients (Fig. 4(a)). The photon loss for skimmed milk can be analyzed by varying the internal coefficient. Based on the graph in Fig. 4(b), when  $g$  increases until 0.8, the photon loss increases gradually and starts to decrease when  $g$  is larger than 0.8. The measured photon loss for anisotropy parameter,  $g$  approaches 1 is lower than the  $g$  approaches 0. Fig. 4(c) and (d) distinguish skimmed milk and full milk in terms of photon count and photon loss.

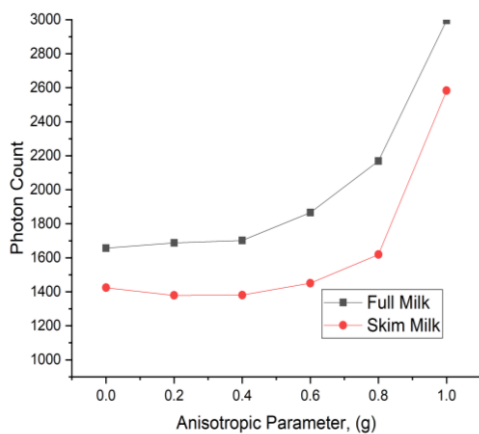
Based on both graphs, forward photon count in full milk is higher than skimmed milk whereas the photon loss in skimmed milk is lower than in full milk. This is due to the fact that skimmed milk has less fat globules than full milk. The large fat molecules in full milk absorb and scatter more light over skimmed milk.



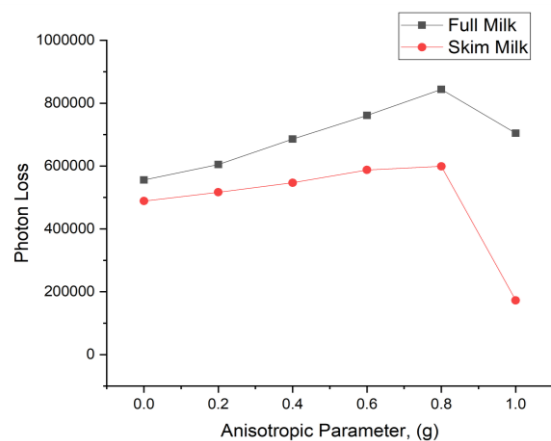
(a)



(b)



(c)



(d)

Fig. 4. (a) Forward photon count of skimmed milk (b) Photon loss with various internal coefficients measured in skimmed milk (c) Photon count for skimmed milk and full milk (d) Photon loss for skimmed milk and full milk.

Stocker *et al.* [27] have done simulation using scattering coefficient,  $\mu_s$  and reduced scattering coefficient,  $\mu_s'$  at different wavelength for untreated and treated raw milk with Ethylenediaminetetraacetic acid, EDTA based on integrating sphere measurements. The scattering properties and refractive index depend on the size of milk fat droplet, where, a high fat globule yields a high refractive index as well as scattering properties [27]. Thus, numerical modeling based on Monte Carlo can support the experimental results where the light propagation in milk is analyzed theoretically in terms of photon count and photon loss.

#### 4. CONCLUSIONS

The milk fat analysis in skimmed and full milk is done based on light propagation in milk. All experimental measurements are done using NIR, VIS and FTIR spectrometers. Full milk sample shows the highest absorbance due to high fat globule in full milk compared to others. A large particle of fat globule inside the medium can provide high absorbance at certain wavelength which specifies chemical properties of water and unsaturated fatty acid. The numerical modeling based on Monte Carlo shows that full milk has higher photon loss and forward photon count than skimmed milk. The higher internal coefficient in full milk results in higher photon count and photon loss. Full milk sample has higher photon count and photon loss due to higher absorption and scattering in the sample. This study can be used to assist the authority to monitor milk adulteration issue to ensure good human well-being.

#### CONFLICT OF INTERESTS

The authors have declared no conflict of Interests.

#### REFERENCES

1. Meretska, M. L., Uppu, R., Vissenberg, G., Lagendijk, A., Ijzerman, W. L., and Vos, W. L., "Analytical Modeling of Light Transport in Scattering Materials with Strong Absorption", *Optics Express*, Vol. 25, No. 20, pp. A906-A921, 2017.
2. [https://www.nbi.dk/~ogendal/personal/lho/LS\\_brief\\_intro.pdf](https://www.nbi.dk/~ogendal/personal/lho/LS_brief_intro.pdf), (Accessed 10/10/2020).
3. Sathish, P., and Gandla, S., "Smart Water Quality Monitoring System with Cost-Effective using IoT", *Heliyon*, 6, 2020.

4. Abegaõ, L. M. G., Alessandra, A. C. P., Sergio, C. Z., Marcio, A. R. C. A. and Jose, J. R. J., "Measuring Milk Fat Content by Random Laser Emission", *Scientific Reports*, Vol. 6, pp. 4-7, 2016.
5. Du, L., Lu, W., Gao, B., Wang, J., and Yu, L., "Authenticating Raw from Reconstituted Milk Using Fourier Transform Infrared Spectroscopy and Chemometrics", *Journal of Food Quality*, Vol. 2019, 2019.
6. Malacarne, M., Andrea, S., Mauro, P., Giorgio, Z., Giulio, V., Martino, C., Giuseppe, B., and Massimo, D. M., "Investigation on the Effectiveness of Mid-Infrared Spectroscopy to Predict Detailed Mineral Composition of Bulk Milk", *Journal of Dairy Research*, Vol. 85, No. 1, pp. 83-86, 2018.
7. Montemurro, M., Schwaighofer, A., Schmidt, A., Culzoni, M. J., Mayer, H. K., and Lendl, B., "High-Throughput Quantitation of Bovine Milk Proteins and Discrimination of Commercial Milk Types by External Cavity-Quantum Cascade Laser Spectroscopy and Chemometrics", *Analyst*, Vol. 144, No. 18, pp. 5571-5579, 2019.
8. Katsumata, T., Aizawa, H., Komuro, S., Ito, S., and Matsumoto, T., "Quantitative Analysis of Fat and Protein Concentrations of Milk Based on Fibre-Optic Evaluation of Back Scattering Intensity", *International Dairy Journal*, Vol. 109, p. 104743, 2020.
9. Amr, M., Sabry, Y. M., Khalil, D., "Near-Infrared Optical MEMS Spectrometer-Based Quantification of Fat Concentration in Milk." *National Radio Science Conference, NRSC, Proceedings*, Vol. 3, No. 3, pp. 409-416, 2018.
10. Vašková, H., Bučková, M., Zálešáková, L., "Spectroscopic Analysis of Milk Fat and Its Mathematical Evaluation", *International Journal of Biology and Biomedical Engineering*, Vol. 10, pp.168-175, 2016.
11. Ouhaddouch, H., Cheikh, A., Idrissi, M. O. B., Draoui, M., and Bouatia, M., "FT-IR Spectroscopy Applied for Identification of a Mineral Drug Substance in Drug Products: Application to Bentonite", *Journal of Spectroscopy*, Vol. 2019, ID 2960845, 2019.
12. Chandra, S., "Fourier Transform Infrared (Ft-Ir) Spectroscopic Analysis of *Nicotiana Plumbaginifolia* (Solanaceae)", *Journal of Medical Plant Study*, Vol. 7, No.1, pp. 82-85, 2019.
13. Prah, S. A., and Keijzer, M., "A Monte Carlo Model of Light Propagation in Tissue", *Dosimetry of Laser Radiation in Medicine and Biology I*, pp. 102-111, 1989.
14. Vinckenbosch, L., Lacaux, C., Tindel, S., Thomassin, M., and Obara, T., "Monte Carlo Methods for Light Propagation in Biological Tissues", *Mathematical Biosciences*, Vol. 269, pp. 48-60, 2015.
15. Song, S., Kobayashi, Y., and Masakatsu, G. F., "Monte-Carlo Simulation of Light Propagation Considering Characteristic of Near-Infrared LED and Evaluation on Tissue Phantom", *Procedia CIRP* 5, pp. 25-30, 2013.
16. Bocklin, C., "Modeling of Light Propagation in Tissue", *ETH Zurich Research Collection*, Vol. 9, No. 2, 2014.

17. Romanov, O. G., Tolstik, A., Velez, F. F., Quijano, N. O., Garcia, I. S., and Diego, J. L. A., "Modeling of Light Propagation in Turbid Media: Application to Biological Tissues", *Nonlinear Phenomena in Complex Systems*, Vol. 15, No. 4, pp. 395-402, 2012.
18. Jain, P., and Sarma, S. E., "Light Scattering and Transmission Measurement Using Digital Imaging for Online Analysis of Constituents in Milk", *Proceedings, Optical Measurement Systems for Industrial Inspection IX, SPIE Optical Metrology, Germany*, 2015.
19. Forcato, D. O., Carmine, M. P., Echeverria, G. E., Pecora, R. P., and Kivatinitz, S. C., "Milk Fat Content Measurement by a Simple UV Spectrophotometric Method: An Alternative Screening Method", *Journal of Dairy Science*, Vol. 88, No. 2, pp. 478-481, 2010.
20. Mahmoud, F. F., El-Shafei, A. G., Abdelrahman, A. A., and Attia, M. A, "Finite Element Modeling of Large Deformation Viscoelasti Frictional Contact Systems", *Journal of Engineering and Applied Science*, Vol. 59, No. 1, pp. 65-85, 2012.
21. Botros, A. Z., and Nasr, K. M. A., "Finite Difference Time Domain in One Dimension Remote Sensing", *Journal of Engineering and Applied Science*, Vol. 47, No. 3, pp. 587-605, 2000.
22. Tsenkova, R., Atanassova S., Itoh, K., Ozaki, Y., and Toyoda, K., "Near Infrared Spectroscopy for Biomonitoring: Cow Milk Composition Measurement in a Spectral Region from 1,100 to 2,400 Nanometers", *Journal of Animal Science*, Vol. 78, No. 3, pp. 515-522, 2000.
23. Prael, S. A., Van Gemert, M. J., Welch, A. J., "Determining the Optical Properties of Turbid Media by Using the Adding-Doubling Method", *Applied Optics*, Vol. 32, No. 4, pp.559-68, 1993.
24. Golshan, A. M., Tarei, M. G., Ansari, M. A., and Amjadi, A., "The Propagation of Laser Light in Skin by Monte Carlo- Diffusion Method: A Fast and Accurate Method to Simulate Photon Migration in Biological Tissues", *Journal of Laser in Medical Science*, Vol. 2, No. 3, pp. 109-114, 2011.
25. Ding, H., Nguyen, F., Boppart, S. A., and Popescu, G., "Optical Properties of Tissues Quantified by Fourier-Transform Light Scattering", *Optics Letters*, Vol. 34, No. 9, pp. 1372-1374, 2009.
26. Qin, J., and Lu, R., "Measurement of the Absorption and Scattering Properties of Turbid Liquid Foods Using Hyperspectral Imaging", *Applied Spectroscopy*, Vol. 61, No. 4, pp. 388-396, 2007.
27. Stocker, S., Foschum, F., Krauter, P., Bergmann, F., Hohmann, A., Happ, C. S., and Kienle, A., "Broadband Optical Properties of Milk", *Applied Spectroscopy*, Vol. 71, No. 5, pp. 951-962, 2017.